We are IntechOpen,
the world's leading publisher of
Open Access books
Built by scientists, for scientists

4,800

Open access books available

122,000

International authors and editors

135M

Downloads

Our authors are among the

154

Countries delivered to

TOP 1%

most cited scientists

12.2%

Contributors from top 500 universities

CLARIVATE ANALYTICS
BOOK CITATION INDEX
INDEXED

WEB OF SCIENCE™

Selection of our books indexed in the Book Citation Index
in Web of Science™ Core Collection (BKCI)

Interested in publishing with us?
Contact book.department@intechopen.com

Numbers displayed above are based on latest data collected.
For more information visit www.intechopen.com

Effects of Radiation on Optical Fibers

Fuhua Liu[1,2], Yuying An[1], Ping Wang[2], Bibo Shao[2] and Shaowu Chen[2]
[1]School of Technical Physics, Xidian University
[2]Key Laboratory of Laser Interaction with Matter,
Northwest Institute of Nuclear Technology
China

1. Introduction

Optical fibers have many advantages over metallic lines such as broad bandwidth, low-loss, immunity from interference due to electromagnetic induction, etc. They can be used to implement ultra-fast pulse signal transmission over a long distance under the circumstance with sophisticated electromagnetic radiation. However, while optical fibers are exposed in nuclear radiation environments, changes in their optical properties will occur thus resulting in deterioration of system performance eventually. Optical fibers will be required to withstand exposure to nuclear environments. Since optical fibers were applied in nuclear radiation environments as signal transmission media, people began to study effects of radiation on optical fibers, to measure the changes of optical fiber parameters, e.g. radiation-induced loss, irradiation damage recovery time and to analyze the effecting factors (Mattern et al., 1974; Evans et al., 1974; Golob et al., 1977; Friebele et al., 1978, 1979, 1980). Research results are used to evaluate the variation degree of optical fiber system performance and their working lives under nuclear circumstance, and to search methods for reducing radiation-induced loss (Tsunemi et al., 1986; Akira et al., 1988). As a result, anti-radiation optical fibers are developed subsequently. With the application of anti-radiation optical fibers, the degradation of performance will be reduced and the system life will be extended accordingly. On the other hand, radiation detecting systems based on the parameter changes above-mentioned are established to monitor the ambient radiation doses of underground nuclear exploders, space-aircrafts, radiation reactors and other nuclear facilities (Ramsey et al., 1993; Moss et al., 1994; Tighe et al., 1995; Fernadndez et al., 2002; May, 2006).

When radiation projects to optical fibers, three effects will produce: (1) Increase of optical fibers absorption loss. The additional loss caused by radiation of photons and electrons with lower energy corresponds with the mechanism of color center. The color center spectrum lies usually within the visible and near-infrared wavelength regions, and it is resonant absorption that leads to additional loss. Neutron or alpha particle radiation absorbed by optical fibers can also cause additional loss. It will mainly damage optical fiber matrix structure and produce atomic structure defects and release electrons. (2) Changes of optical fiber refractive index. As a result, boundary conditions will no longer fully meet the optical fiber waveguides, and increase of evanescent field coupling energy will lead to additional loss. (3) Development of optical fiber luminescence. It is usually considered to be fluorescence or Cerenkov effects. It is very difficult to detect the light due to its weak intensity along optical fiber axis.

The purpose of the research is to provide experimental data for reducing radiation-induced loss of optical fibers and to attempt to evaluate system performance degradation of optical fibers under nuclear environments.

This chapter will mainly discuss transient γ-ray effects on commercial optical fibers. Two different dose and dose rate γ-ray pulses are employed to irradiate four types of optical fibers and radiation-induced losses are measured by using five lasers with different wavelengths as carriers.

2. Effects of γ-ray radiation on optical fibers

2.1 Loss mechanism of optical fibers

Loss is inherent nature of optical fibers. In accordance with different generation mechanisms, loss is usually classified into: absorption loss, scattering loss, waveguide loss and bending loss, etc (Liu et al., 2006). When light-waves propagate in optical fiber media, interactions between photons and atoms occur. Photons will continue to transfer their energy to matrix atoms gradually. This process results in absorption loss. Optical matrix materials and impurities are the main factors influencing the absorption loss. Based on the different absorption subjects, absorption loss is classified into intrinsic absorption loss, impurity absorption loss and atomic defect absorption loss. Collisions of photons with substrate atoms, microscopic changes in optical fiber material density, and uneven composition distribution or structural defects generated during the manufacturing process will produce scattering loss. Rayleigh scattering which is inevitable is the lowest limit of optical fiber loss. Once variation of boundary condition for optical waveguide or waveguide deformation appears, part of light-wave mode energy will leak out, resulting in energy loss, i.e. waveguide loss. Fiber bended to a certain extent, part of the light energy will be lost, resulting in bending loss.

2.2 Effects of γ-ray radiation on optical fibers

The photon of γ-ray is the quantum of electromagnetic radiation. Radiation damage of material due to incident photon flux is varied, depending upon the material through which the photon propagate and the photon energy of the radiation. Damage ranges from simple heating, as photons are absorbed, to ionization and even photon-nuclear disintegration if the interacting photon energy is of the order of 10MeV or greater. According to different photon energy, effects of γ-ray on materials include: photoelectric, Compton, electron pair and scattering effects (Mei, 1966). The variation of cross sections for different effects in optical fibers with photon energy is calculated by GEANT4 and shown in Fig. 1. The data exhibited in Fig. 1 serve to point out that Compton Effect is dominant over the behavior with γ-ray radiation exposure on optical fibers. In addition, there is also fluorescence and Cerenkov effects. The penetration of radiation into materials is not only dependent upon the material itself but also upon the type of radiation. The penetration rate of γ-ray into optical fibers is calculated and shown in Fig.2. Atomic and molecular electron energy levels are on the order of a few electron volts, and so an electron bound at an atomic site in a material would not undergo a simple transition to a higher atomic energy level due to interaction with γ-ray. The resulting high energy electron of Compton Effect is the primary source of radiation damage due to γ-ray absorption in optical fibers. Its energy and intensity distribution in the horizontal profile of optical fibers is depicted in Fig.3, 4, and 5 when γ-ray with photon energy of 0.3, 0.8, and 1.0MeV projects along the vertical profile respectively.
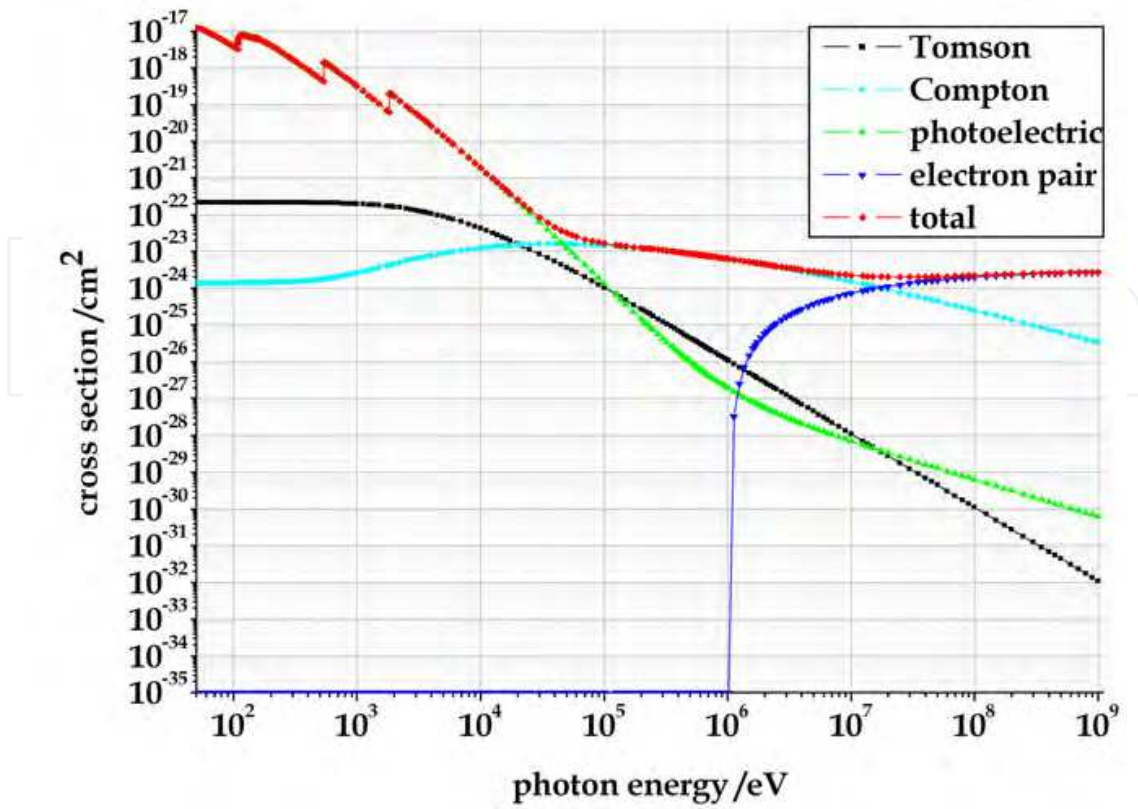
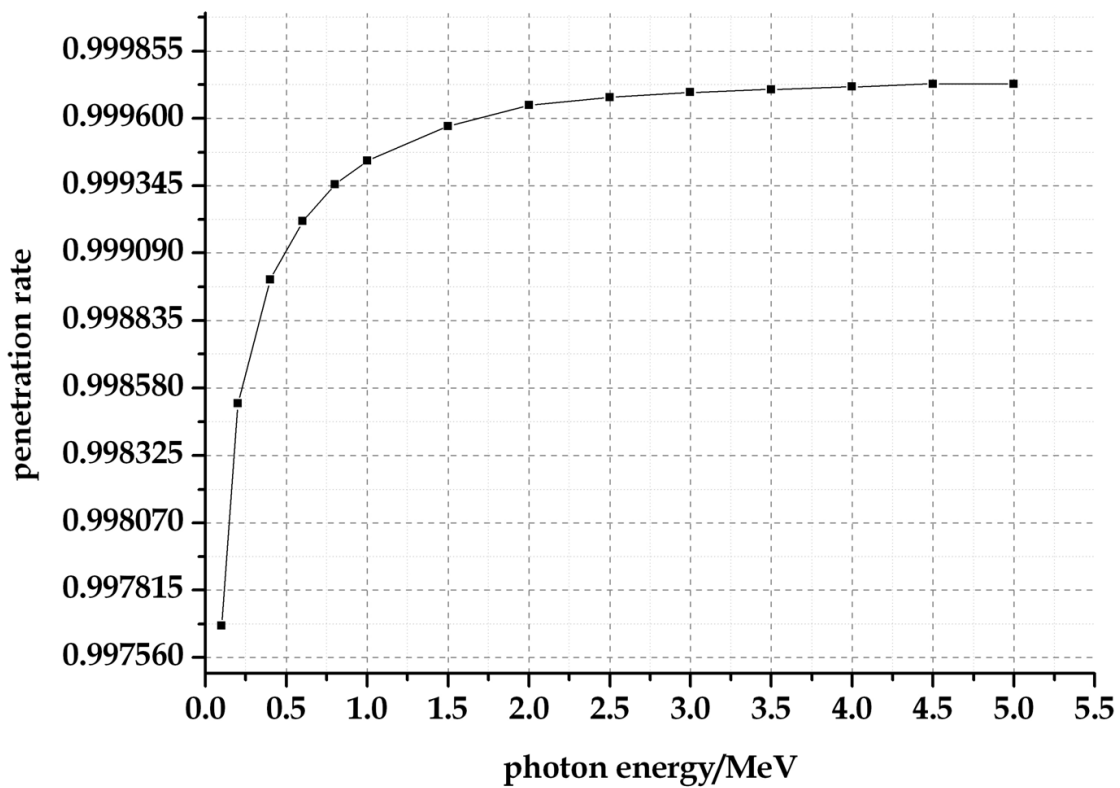Fig. 1. Curve of different effects cross sections varying with photon energy.

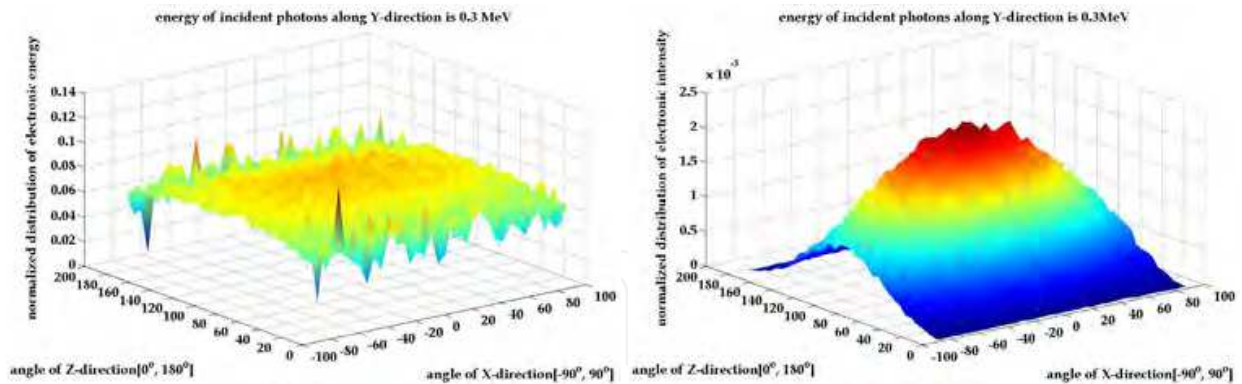Fig. 2. Graph of penetration rate of γ-ray into optical fibers as a function of photo energy.

Fig. 3. Diagrams depicting distribution of resulting electronic energy and intensity in horizontal profile of optical fiber while photo energy of γ-ray is 0.3MeV.
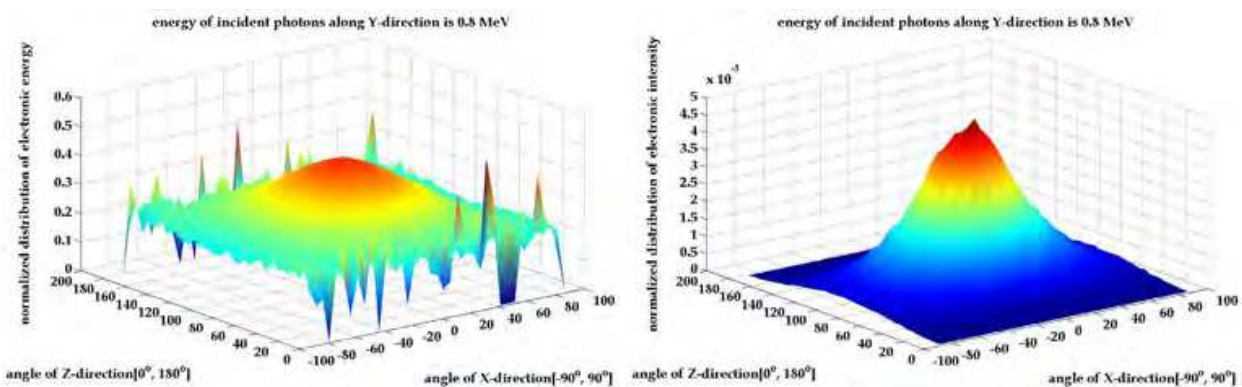

Fig. 4. Diagrams depicting distribution of resulting electronic energy and intensity in horizontal profile of optical fiber while photo energy of γ-ray is 0.8MeV.
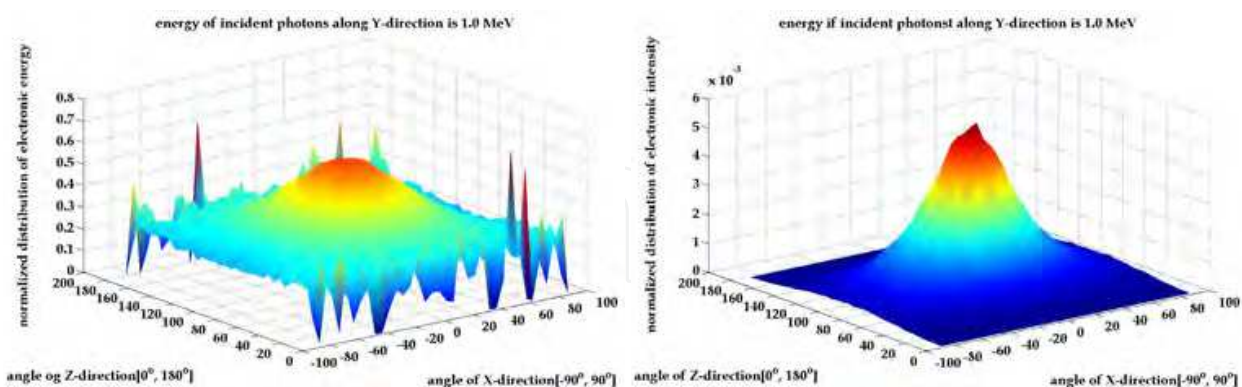

Fig. 5. Diagrams depicting distribution of resulting electronic energy and intensity in horizontal profile of optical fiber while photo energy of γ-ray is 1.0MeV.

If sufficient ionizing radiation of γ-ray with energies from several MeV down into the keV range is absorbed by optical fibers, it causes damages to optical fiber materials. The damages which produce additional radiation-induced loss on light propagation are associated with the energy and intensity distribution of the resulting high energy electrons.

2.3 Mode distribution and alteration of refractive index in optical fibers

The index of refraction is attributable to the electromagnetic properties of optical fibers. As in crystalline, similar processes of color center formation by radiation absorption may occur in amorphous. It's reasonable to assume that some changes in the index of refraction may result from radiation exposure. In fact radiation-induced changes in the refractive index distribution of optical fibers will influence distribution of mode field and confinement factor and bring additional waveguide loss. Optical waveguide loss arises from the waveguide imperfections. Confinement factor of waveguide can be described as (1) (Yasuo, 2002)

$$\Gamma = \frac{V + \sqrt{b}}{V + \frac{1}{\sqrt{b}}} \tag{1}$$

where b is the normalized propagation constant, $b = \frac{(\beta / k_0)^2 - n_2^2}{n_1^2 - n_2^2}$. V is the normalized frequency, $V = k_0 n_1 a \sqrt{n_1^2 - n_2^2}$. k_0 is the propagation constant of plane wave in vacuum, $k_0 = \omega \sqrt{\varepsilon_0 \mu_0}$. a is the radius of the core. ω is the angle frequency of light-wave.

The computational results of relative mode field distribution in the core and clad of optical fibers, relative distribution of electric field intensity and confinement factors as a function of refractive index changes are shown in Fig.6, 7, 8 respectively. Any alteration in indexes of refraction within optical waveguide will influence the mode distribution and cause waveguide loss eventually.
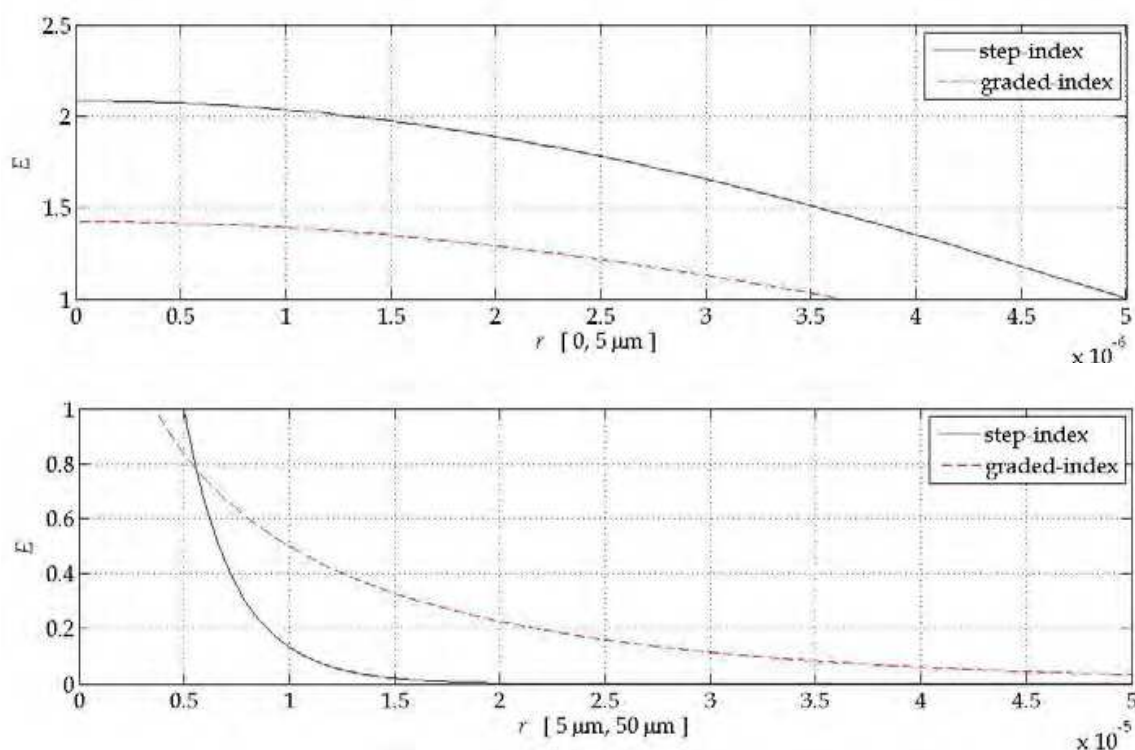

Fig. 6. Relative mode field distribution of electromagnetic wave in core and clad.
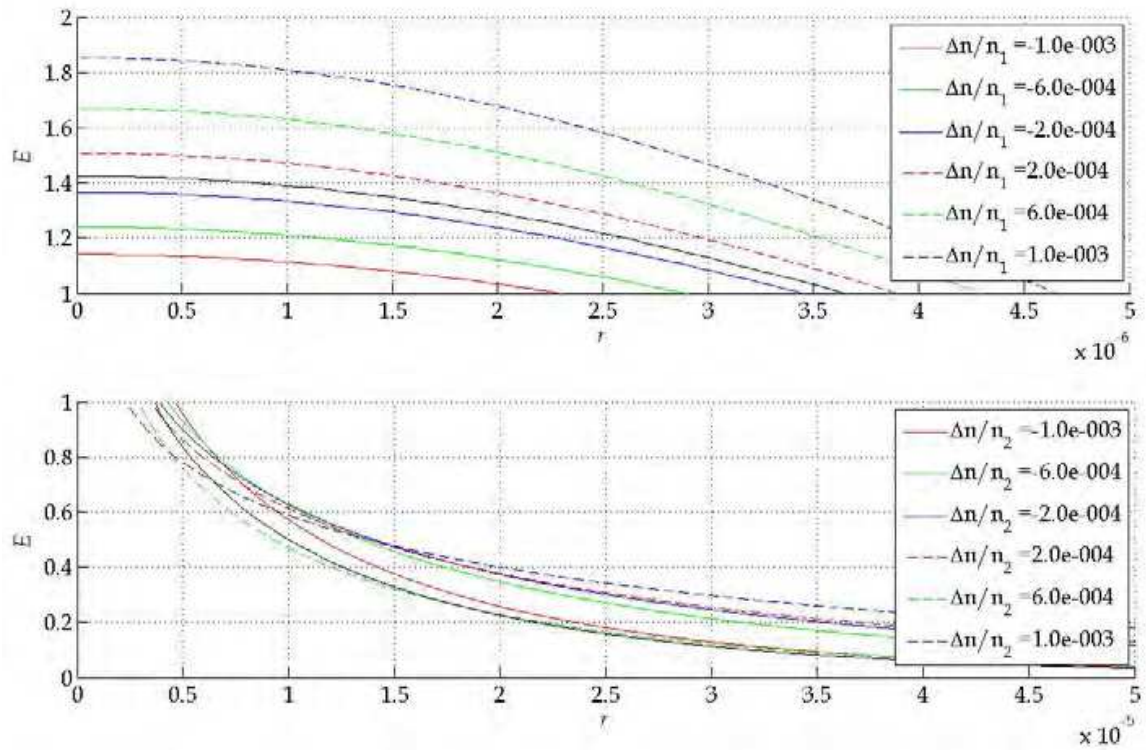
Fig. 7. Relative distribution of electric field intensity in optical fiber as a function of refractive index changes.
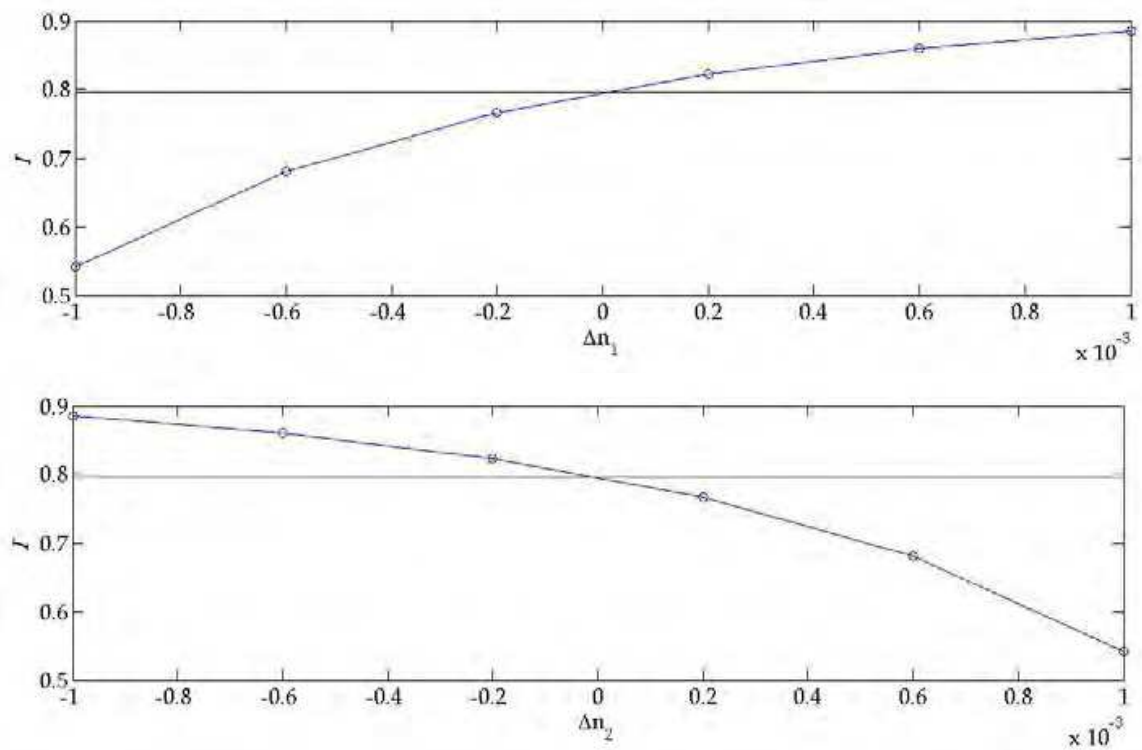

Fig. 8. Confinement factors as a function of refractive index changes.

3. Design of experimental measurement system

3.1 Measurement system structure

In order to measure pulsed γ-ray radiation-induced loss, a special experimental measurement system will be needed. During the system design, the following factors should be considered comprehensively: (1) Radiation sources. Radiation dose is adjusted by the nature of ray attenuations, with real-time simultaneous multi-point monitoring. (2) Optical fibers. In order to obtain uniform irradiation, optical fibers are coiled into circles with diameters as small as possible e.g. several centimeters, until the bending loss cannot be neglected. Its exposure length can be adjusted conveniently. (3) Response and record time sequence. The system's response time should be controlled within a tenth or less of the time width of the radiation rays in order to reduce influence of the measurement system time characteristics on results. To ensure records of effect signal waveforms, all devices should be set at automatic working states. The measurement system linear dynamic range of amplitude should be as large as possible e.g. 100. (4) Measurement environment. The main radiation source is a large electron accelerator with strong space electromagnetic radiation, so all the electronic equipments should be shielded effectively.

A typical experimental apparatus for measuring the radiation-induced loss in optical fibers is shown in Fig. 9.

3.2 Measurement system components

The measurement system consists of three parts: (1) Signal recording section. It contains a trigger, a signal generator and a transient digital oscilloscope. The trigger is used to start the transient oscilloscope and signal generator simultaneously. The signal generator is used to produce pulse signal to drive the analog optical fiber transmission system, thus producing pulsed light signal. The transient oscilloscope is used to record the optical signal while γ-ray impulses on optical fibers. (2) Optical fiber transmission section. It contains a semiconductor laser transmitter and a receiver. The semiconductor laser is used to convert the pulsed electric signal into optical ones, and the semiconductor receiver is used to convert pulsed light signals into electrical ones and send it to the transient oscilloscope. (3) Target section. It contains optical fibers under test and regulating facilities.
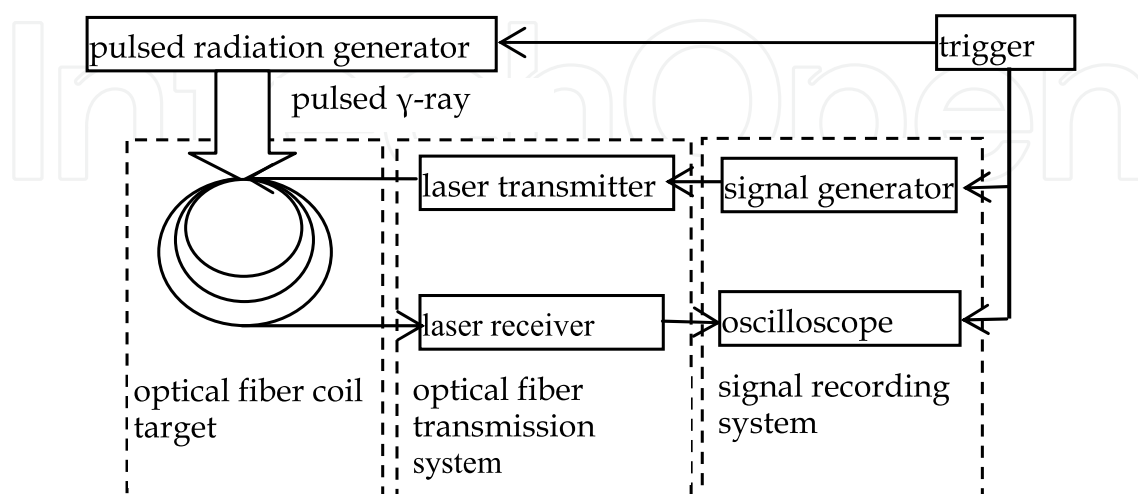

Fig. 9. Schematic diagram of experimental setup for measuring transient radiation-induced loss in optical fibers under pulsed exposure.

3.3 Main technical parameters

A comprehensive list of the important parameters in conducting a measurement of the radiation response of optical fibers is as below:

Radiation source I: average photon energy of 0.3 MeV, pulse width of 25ns, dose rate of 2.03×10^7 Gy/s.

Radiation source II: average photon energy of 1.0 MeV, pulse width of 25ns, dose rate of 5.32×10^9 Gy/s

Trigger: input/output of -10-+10 V adjustable, time interval of 0.001-10µs adjustable.

Signal generator: input and output amplitude of -5-+5 V adjustable, pulse width of 0.0003-10µs adjustable.

Transient oscilloscope: analog bandwidth of 1 GHz, digital sampling rate of 5 GHz.

Optical fiber transmission system: bandwidth of 3 GHz, in-band flatness within ±1dB, linear dynamic range of 100 (non-linear is less than 3%), peak output noise less than 5mV. input / output impedance of 50 Ω, the laser wavelength of 405, 660, 850, 1310 and 1550 nm.

Optical fiber types: ITU G.651(50/125µm, 62.5/125µm), G.652 and G.655 available bare optical fibers.

In considering the effect of radiation, the radiation damage is a dynamic process, i. e. concurrent with the darkening due to the production of color centers by the irradiation is recovery due to emptying of the holes and electrons out of these centers. Thus ,the net optical absorption that is observed is the sum of these two process.

4. Development of laser transmitter and receiver

A broad-bandwidth analog optical fiber transmission system is developed for radiation-induced loss measurement under the circumstance with complicated electromagnetic fields. The ultra-fast pulsed electric signal is converted to optical by electro-optic conversion method. With certain kilometers propagation, the optical signal is recovered by photo-electric conversion method. The experimental measurement results of the transmission system indicate that its bandwidth is (0.0003-3)GHz, in-band flatness ±1dB, linear dynamic range 100, output peak-to-peak noise less than 5mV, and input/output standing-wave-ratio less than 2.

4.1 Structure and design
4.1.1 Structure

An analog optical fiber transmission system is usually comprised of a transmitter, a certain distance long optical fibers and a receiver. The structure is shown in Fig. 10.
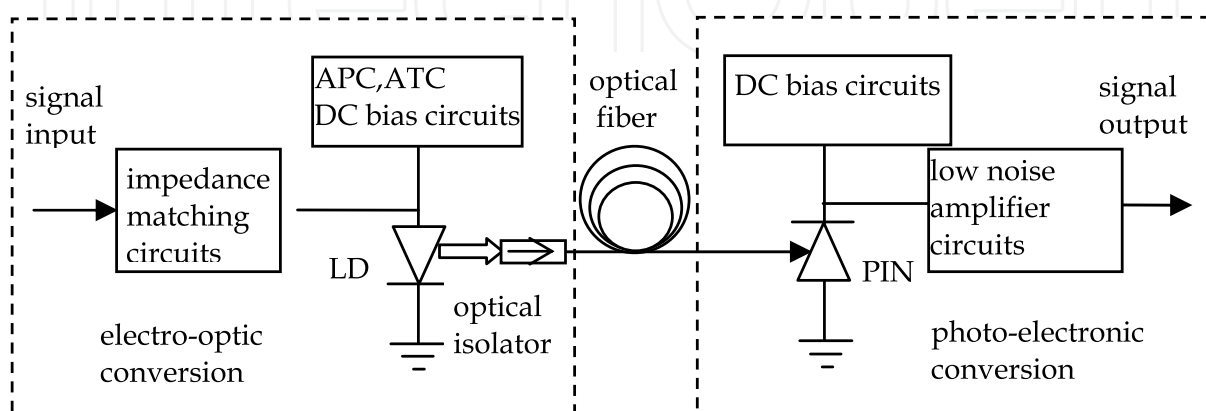

Fig. 10. Schematic diagram of broad bandwidth analog optical fiber transmission system.

Key technologies for designing and fabricating a broad bandwidth analog optical fiber transmission system lie in these aspects: (1) By impedance matching, the response in high frequency band is compensated and the overall system bandwidth is expanded consequently. (2) With peak-to-peak noise of PIN photoelectric diode and preamplifier reduced, the linear dynamic range is extended. (3) The parasitic parameters of components and micro-striplines in the modules reduced, the system can operate stably.

4.1.2 Transmitter

The transmitter contains an integrated multi-quantum-well distributed feedback laser diode(MQW-DFB-LD), an optical isolator, automatic power control (APC) circuits (Tanaka et al., 2002; Zivojinovic et al., 2004; Pocha et al., 2007), automatic temperature control (ATC) circuits, and DC bias circuits. The potential improvements of overall optical system performance depend on studying and analyzing LD transient characteristics such as modulation bandwidth, intensity, frequency noise levels and nonlinear distortion. Numerical laser models and sophisticated computation can accurately predict LD transient characteristics of above-mentioned parameters. The time dependent carrier density rate equations for LD in the active region are described as (Huang, 1994; Ghoniemy et al., 2003):

$$\frac{dN}{dt} = \frac{J_e}{ed} - \frac{N}{\tau_e} - GP(N - N_{leak}) \tag{2}$$

$$\frac{dP}{dt} = GP(N - N_{leak}) - \frac{P}{\tau_p} + \beta\frac{N}{\tau_e}$$

where N is the average density of electrons, P is the average density of photons, N_{leak} is the density of leaked carriers, d is the thickness of the active layer, τ_e is the lifetime of electrons, τ_p is the lifetime of photons, G is the differential coefficient which expresses light gain, β is the simultaneous emission coefficient, J_e is the injected current density, e is the electron charge.

The cutoff modulation frequency of LD is deduced from (2) and given by

$$fc = \frac{1}{2\pi}\sqrt{\frac{\Gamma N_{leak}G\tau_p + 1}{\tau_e\tau_p}\left(\frac{J_e}{J_{th}} - 1\right)} \tag{3}$$

where, Γ is the light gain confine factor, J_{th} is the threshold current density.

From (3) it can be conclude that the cutoff modulation frequency can be enhanced by increasing the injected current. Considering the carrier transport effects, too large injected current may lead to the variation of the refractive index distribution in the active region, resulting in the deterioration of the modulation performance. The appropriate bias current should be selected by considering the relationship of bandwidth with dynamic range synthetically.

With the help of a light-wave component analyzer, the transient characteristics of LD can be analyzed. The electrical equivalent circuit is shown in Fig. 11. L_{p1}, L_{p2} is the lead inductance, C_p the package parasitic capacitance, C_d the PN junction diffusion capacitance, C_b the PN junction barrier capacitance, R_{diff} the PN junction differential resistance, R_v the bulk resistance of semiconductor material, D the equivalent ideal diode. Elemental parameters in the electrical equivalent circuits provide P-Spice simulation software with original data.
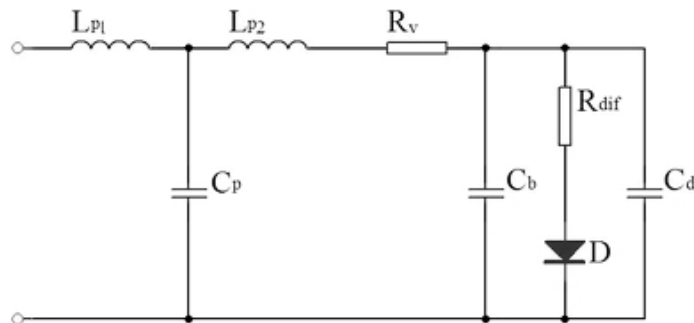
Fig. 11. Equivalent AC circuit diagram of LD.

A basic driving circuit is designed to meet LD analog amplitude modulation, and shown in Fig. 12. In the figure D_1 is designed to prevent LD from reverse breakdown. R_1-R_4, C_1-C_3 are mainly used for impedance matching and high frequency response compensating. L_1, C_4, and C_5 provide the bias decoupling, reducing transient current impact on LD, V_{in} is input modulation signal, and I_{bias} DC bias current.

APC circuits are used to provide LD with static operating point current. Precise temperature control is needed for LD to operate stably, since its threshold current, output power and peak wavelength will vary with junction temperature fluctuation. ATC circuit will meet the demand of junction temperature control. With APC and ATC circuits, the LD's variation of output power keeps within 2%, and the variation of operating temperature keeps within 0.1℃.

There may be some parasitic effects imposed on modulation characteristics to a certain extent. Simulation results show that when a LD is working in high-frequency modulation, the parasitic lead inductance will be impacted obviously on the amplitude-frequency characteristics. Efforts should be made to reduce the distribution parameters to a level as low as possible in different package forms in order to make the LD work stably.
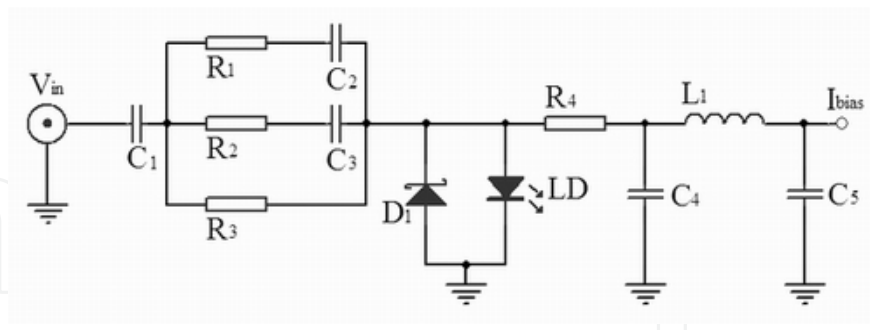

Fig. 12. Principle circuit diagram of impedance matching for electro-optic conversion module.

4.1.3 Receiver

The receiver is comprised of a PIN detector, bias circuit and broad band-width low-noise amplifier. The PIN converts optical signals into electrical ones. The broad bandwidth low-noise amplifier enlarges the signal to an advisable level suitable for recording. Since the PIN output signal is usually weak, such techniques as low-noise, high-gain amplification and impedance matching are needed to design the receiver.

The equivalent PIN AC circuit is shown in Fig. 13 (An, 2002). In the figure I_i is an ideal current source, C_j the junction capacitance, R_j the junction resistance, R_p and C_p equivalent parasitic values, and R_{load} equivalent load for the amplifier. Amplifier bandwidth, noise characteristics, and impedance matching should be taken into account in designing photo-electric conversion module. Its principle circuit is shown in Fig. 14.
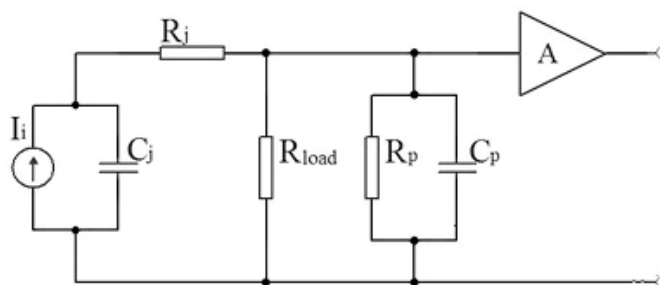

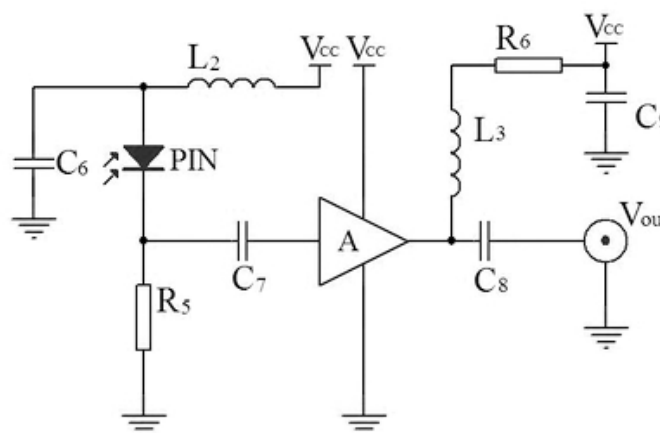Fig. 13. Equivalent AC circuit diagram of PIN detector.

Fig. 14. Principle circuit diagram of photo-electric conversion module.

4.2 Performance
4.2.1 Bandwidth
Bandwidth indicates the response of the input electrical signal frequency components (Hinojosa et al., 2001). Both frequency and time domain measuring methods are employed in the experiments. In frequency-domain measurement a light-wave component analyzer is used. The results show that bandwidth is (0.0003-3) GHz, band flatness ±1dB. The measured amplitude-frequency characteristic curve is shown in Fig. 15 (frequency sweep range (0.0003-3) GHz, amplitude coordinate scale 2 dB/div). With a electrical sub-nanosecond pulse signal generator and a broad bandwidth digital oscilloscope, response in time domain is measured. The typical pulse waveform recorded is shown in Fig. 16. In the figure R1 is input pulse signal wave, and R2 is output waveform. The wave front of R1 and R2 is 153.5ps and 169.1ps respectively. According to the Gaussian approximation formula estimation, its bandwidth is approximately 3 GHz.
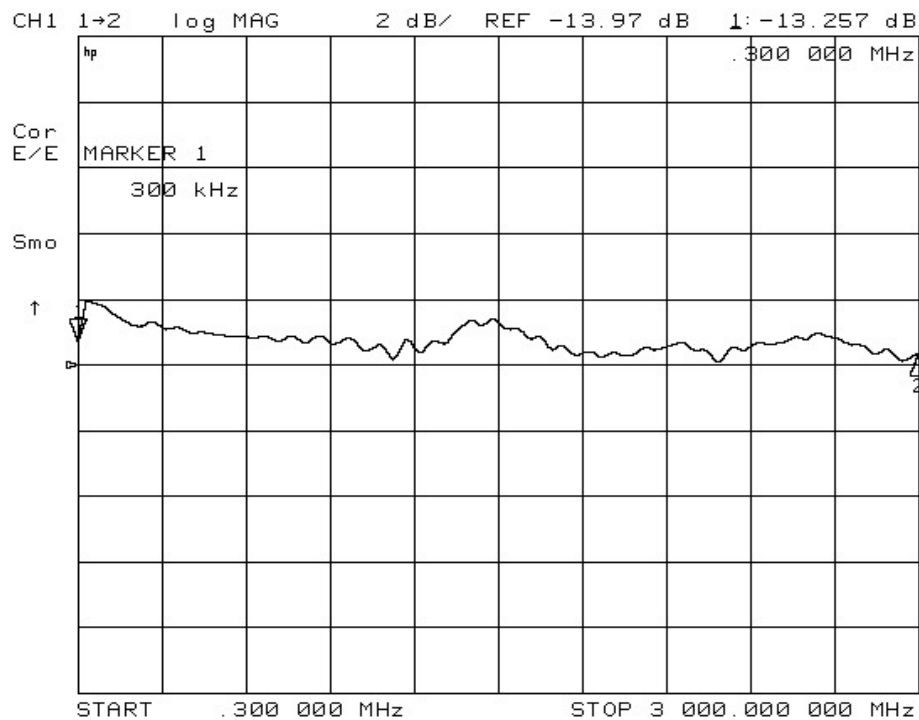
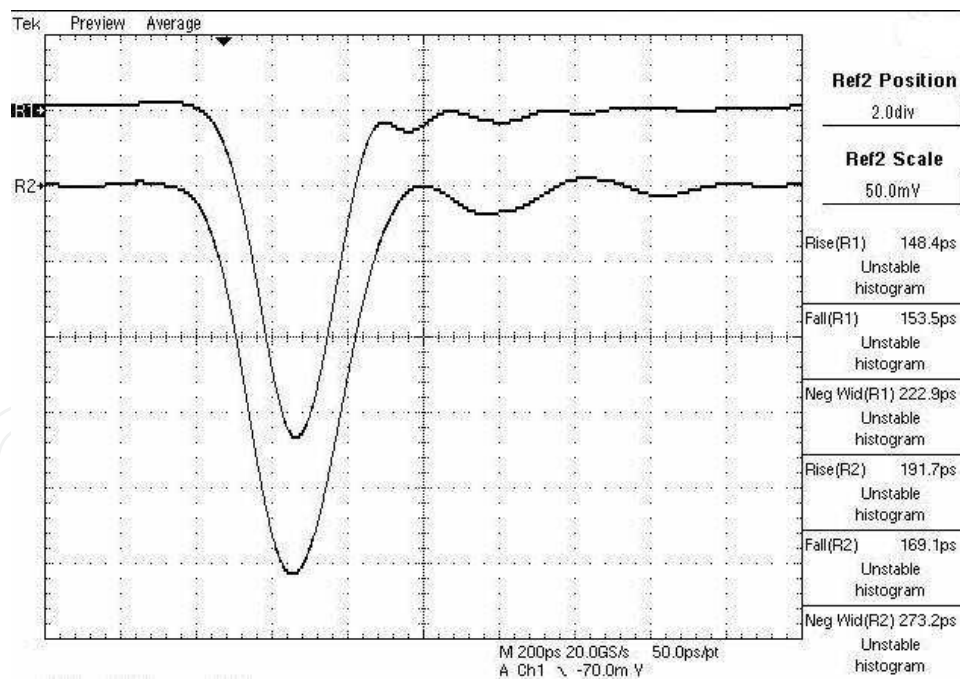Fig. 15. Curve of amplitude-frequency characteristics.

Fig. 16. Waveform of pulse response.

4.2.2 Linear dynamic range

The linear dynamic range of the optical fiber transmission system is measured by point-to-point scanning method. The input/output data and fitting curve are shown in Fig. 8. The result indicates that its dynamic range is greater than 100 with non-linear error less than 3%.
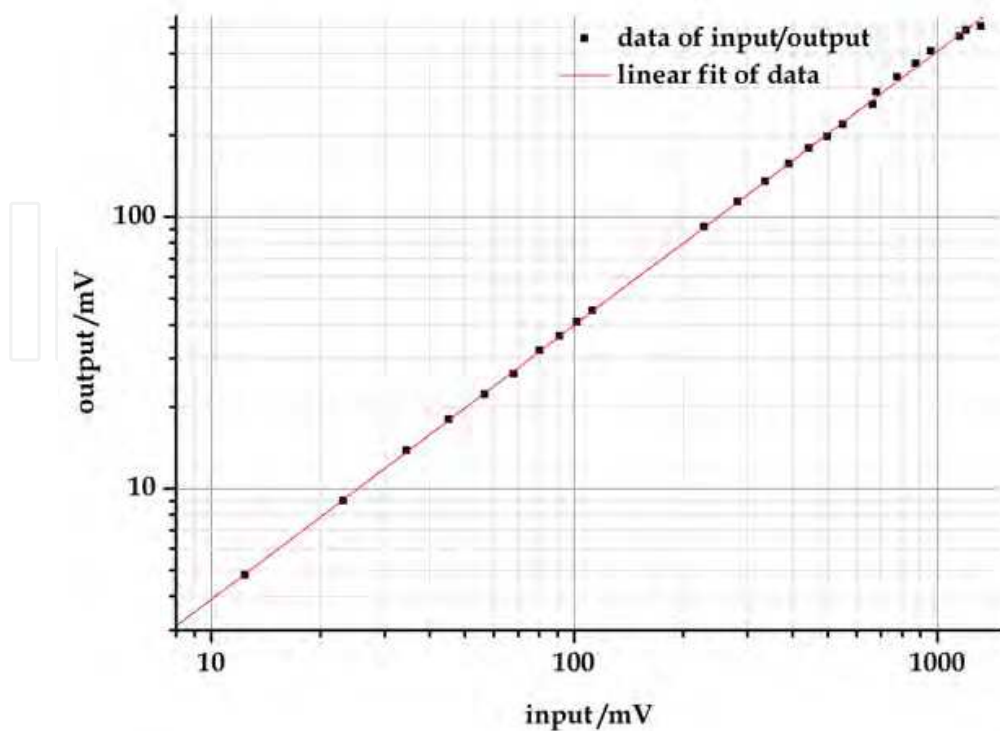
Fig. 17. Data and linear fitting curve of response.

4.2.3 Output noise

A broad bandwidth digital oscilloscope is used to record the output noise while the input is zero. A typical waveform recorded is shown in Fig. 18(time scale of 50ns/div, amplitude scale of 1mV/div). It can be seen from the waveform that the peak output noise V_{p-p} is less than 5mV (3.34mV recorded).
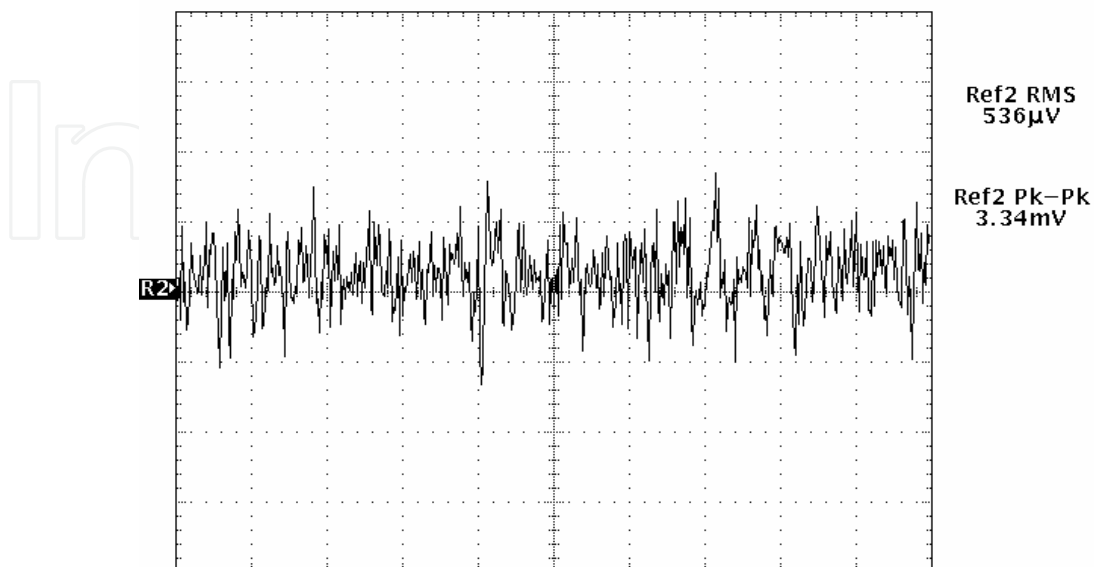

Fig. 18. Waveform of output noise.

4.2.4 Standing wave ratio

By a light-wave component analyzer, the measured curve is shown in Fig. 19. (frequency sweep range of (0.0003-3) GHz, amplitude coordinate scale of 1dB/div). The result shows that SWR is less than 2(1.59 recorded).
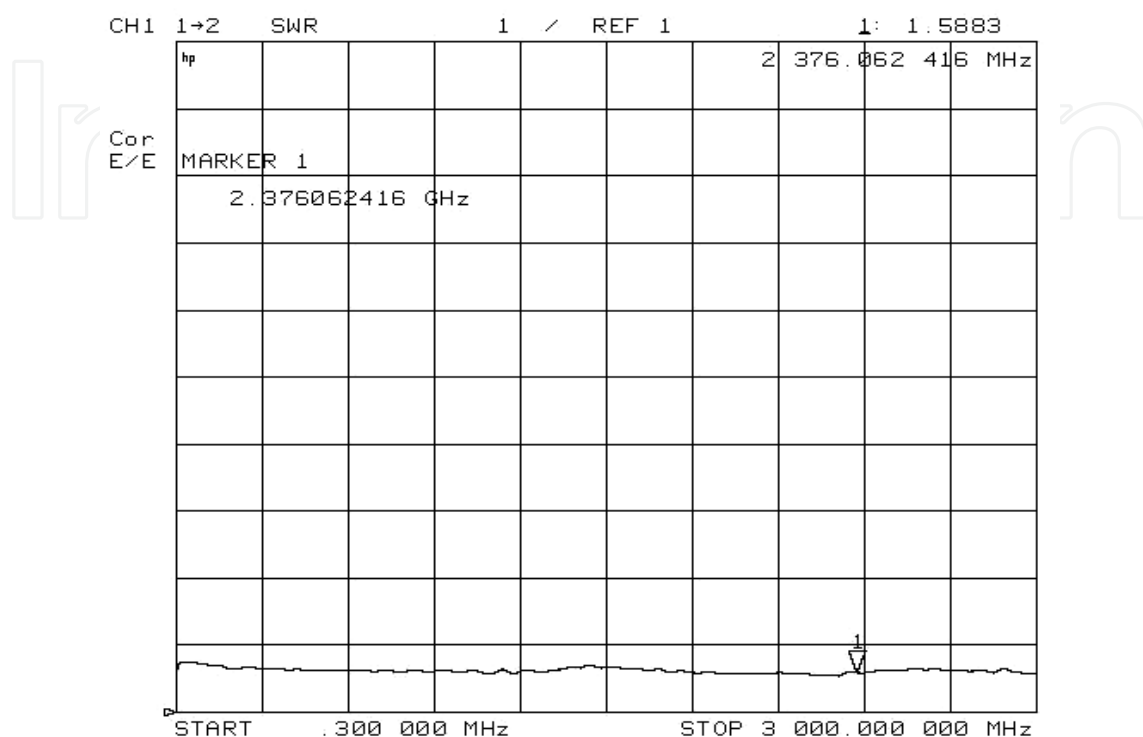

Fig. 19. Curve of standing-wave-ratio in all bandwidth.

5. Results and analysis

Two different kinds of pulsed γ-ray devices with average photon energy of 0.3MeV, pulse width of 25ns, dose rate of 2.03×10^7Gy/s and average photon energy of 1.0MeV, pulse width of 25ns, dose rate of 5.32×10^9Gy are employed as irradiation sources in the experiment. The transient radiation-induced loss of pulsed γ-ray effecting on single-mode and multi-mode optical fibers have been measured. Optical fiber transmission systems with several different wavelength such as 405, 660, 850, 1310 and 1550nm are involved in the experimental measurement system.

5.1 Amplitude performance of transient radiation-induced loss

The experiments have been accomplished on two devices with high/low ray flux respectively. The high flux device makes detection system saturate, which has shorter detection wavelengths (405, 660 and 850nm). The low flux device exerts very low response on detection system which has longer detection wavelength (1310 and 1550nm). The signal level is too low to detect. The average radiation-induced loss of optical fibers under relative low and high flux pulsed γ-rays are shown in Table 1. and 2. respectively. It has become evident that the radiation-induced loss experienced by optical fibers is extremely larger than the intrinsic loss and dependent on the fiber type. It is appear that the single mode fiber may be influenced to a lesser degree than multi mode fibers. It is likely from the difference in

fractions of optical power that propagates within the cladding of the two types of fiber. To the response of same type fiber, the radiation-induced loss relies upon the wavelength of laser carrier. It is obvious that the shorter the wavelength of laser carrier, the larger the radiation-induced loss of optical fiber.

optical fiber types	G.651/50/125		G.651/62.5/125		G.652		G.655	
detection wavelength /nm	1310	1550	1310	1550	1310	1550	1310	1550
radiation-induced loss /dB/m/Gy	0.027	0.016	0.037	0.017	0.023	0.015	0.031	0.011

Table 1. Average transient irradiation-induced loss under low pulsed γ-ray.

optical fiber types	G.651/50/125			G.651/62.5/125		
detection wavelength /nm	405	660	850	405	660	850
radiation-induced loss /dB/m/Gy	6.94	6.34	1.87	7.55	6.92	2.15

Table 2. Average transient radiation-induced loss under high pulsed γ-ray.

5.2 Time performance of transient radiation-induced loss

Typical light signal waveform is shown in Fig. 20. The calculation result shows that the response time of transient radiation-induced loss is approximately 5ns. In order to measure the recovery of the tested optical fibers, the optical spectrum loss at the range of 700-1600 nm is measured and compared with non-irradiated ones. The results are shown in Fig. 21. It can be seen from Fig. 21 that the radiation-induced loss of pulsed γ-ray effecting on optical fibers still remains, especially evident in the range of 700-1000nm and around 1390nm. The permanent radiation-induced loss increases with the decrease of wavelength in this range. To verify the heat recovery of radiation effects, the optical fibers have been heated to 80℃ for 2h and the above-mentioned loss measurements are repeated then. It can be found that the loss have no changes virtually indicating the existence of permanent radiation-induced loss under the irradiation conditions in this experiment.

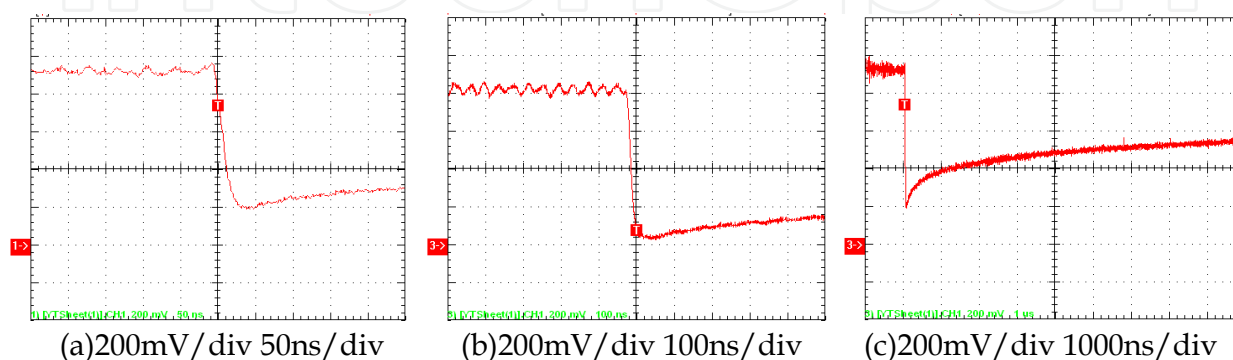(a)200mV/div 50ns/div   (b)200mV/div 100ns/div   (c)200mV/div 1000ns/div

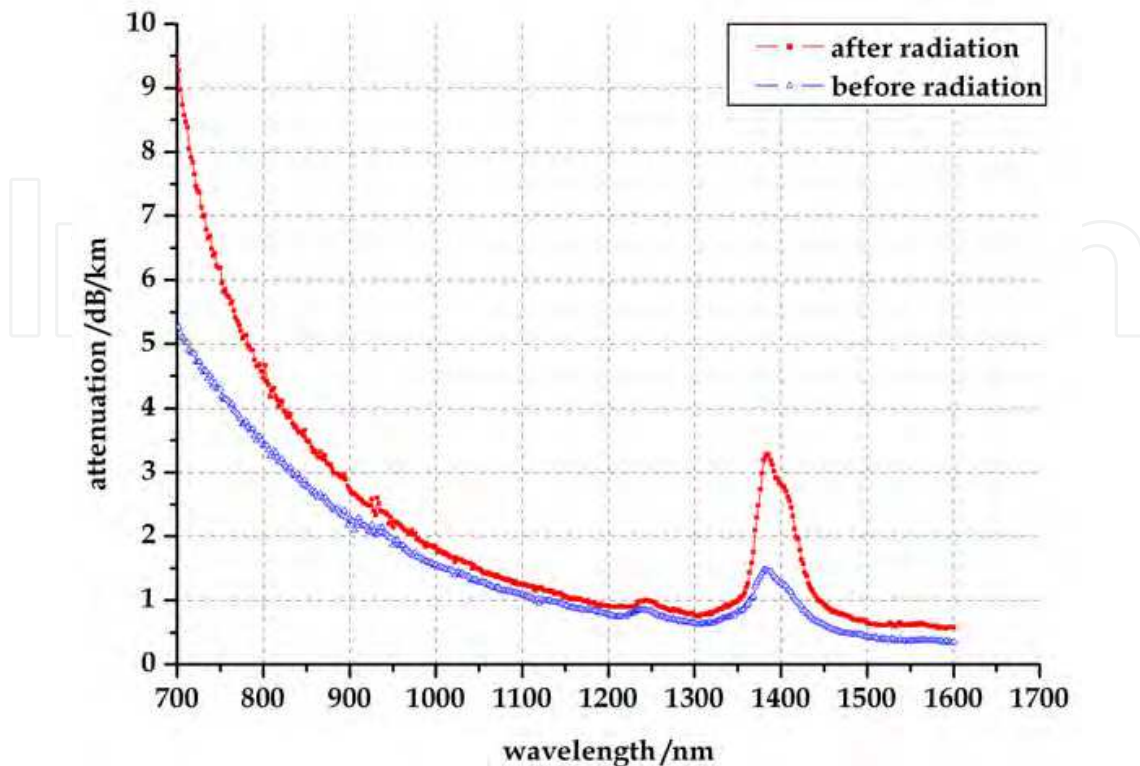Fig. 20. Typical signal waveform recorded in experiments(200mV/div, 50, 100,200ns/div).

Fig. 21. Optical spectrum loss curve comparison before and after radiation exposure.

5.3 Relationship between transient radiation-induced loss and radiation dose

By 850nm laser measurement system, the measured data of low flux γ-ray transient radiation-induced loss on optical fiber G. 651 (62.5/125µm) and fitted curve are shown in Fig. 22. It can be drawn that the transient radiation-induced loss has an approximate linear relationship with total dose in the range of 0.1-3.5 Gy. It is observed that the radiation-induced loss tends to saturation with increasing dose. The saturation is associated with the total radiation-induced color centers in a given length of fiber under test. In the experiments, it is not observed that the decreasing in radiation-induced loss with increasing dose, so called radiation annealing.

Luminescence and Cherenkov lights are not observed in the experiments due to their weak intensities along fiber axis. The sensitivity of the measurement system is to be improved.

5.4 Effect analysis

The essential difference between the crystalline and amorphous solid is that there is not long-range order in the latter. Instead there are localized regions of ordered atomic arrangements in amorphous solids that exist only over a few atomic diameters. Therefore there will be localized electronic states within glasses which account for the optical properties in such materials. A color center is an impurity or imperfection within an otherwise well-ordered system. Generally there will be a set of energy levels available for electronic transitions. These energy levels then represent an absorption spectrum while light not absorbed gives the material its characteristic color. Impurities, atomic defects, irregular

arrangements of atoms or trapped charge carriers can cause color centers to form with sets of specific absorption spectrum.
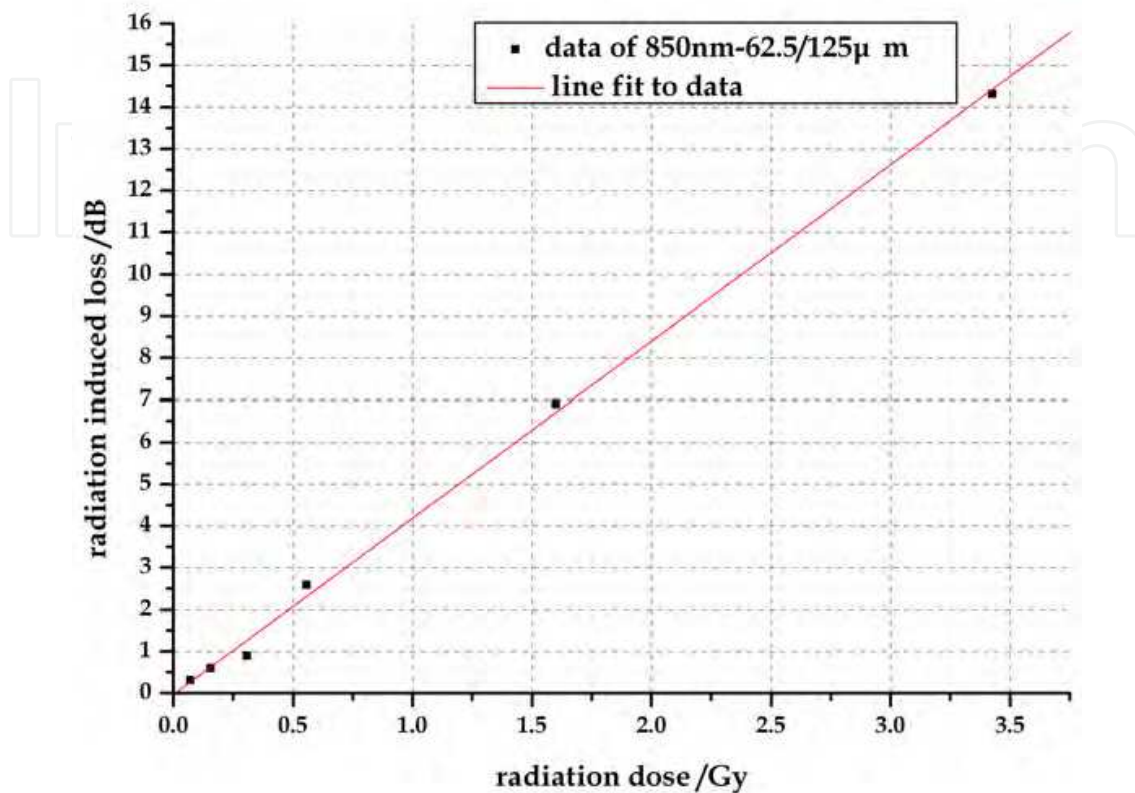

Fig. 22. Experimental data and fitting curve of transient radiation-induced loss.

When γ-ray irradiates on optical fibers, Compton effect will occur usually and the resulting high energy electrons causing the primary radiation damage due to γ-ray absorption in optical fibers. High energy electrons will increase the concentration of color centers, which lead to additional absorption of incident light. Short-lived color center will continue to prevent the formation of new color centers. Therefore in a certain range of radiation dose, radiation-induced loss presents an approximately linear relationship with doses, but as the dose increases, radiation-induced loss tend to get saturated. γ-ray radiation also results in overall optical waveguide deterioration due to changes in the indexes of refraction of core, cladding, or both. It is likely that we could not be able to clearly separate the absorption effect and the index of refraction effect. But in this case, it may be manifest that the absorption effect is dominant.

The role of external heat may accelerate the transition of excitation level, the relaxation of carriers from trapping, or diffusion of color centers, for many forms of color centers are unstable and thermal processes are sufficient to restore the material to its original state. So heat may be beneficial for recovery of radiation-induced loss. But external heat appears invalidation to the permanent radiation-induced loss, which arises from stable color centers.

Radiation-induced loss is somewhat dependent on the fiber types. It appears that the single-mode fibers may be less affected than multi-mode fibers. Single-mode fibers have more concentrated electromagnetic energy distribution than multi-mode fibers. In the same

irradiation conditions, the absorption of single-mode fiber radiation dose is relatively small in the mode distribution region, so the radiation-induced loss of single-mode fiber is lower than that of multimode fiber.

6. Conclusion

In this chapter, two different dose rates of pulsed γ-ray devices are used to irradiate four kinds of optical fibers. By using near infrared and visible wavelength measurement system, the radiation-induced loss is measured. It can be drawn from the experimental results: (1) Under the same experimental condition, the radiation-induced loss of multimode fibers is slightly larger than single-mode fibers. (2) Radiation-induced loss will increase as the detection laser wavelength shifts from near-infrared to visible regions of optical spectrum. Within a certain dose range transient multi-mode fiber radiation-induced loss displays a nearly linear dependence upon the total dose. (3) Two models are invoked to explain radiation-induced loss. One is that the generation of new color centers in fiber materials will increase the absorption loss in the near infrared and visible region. The other is that the changes of refractive index will lead to additional waveguide loss. Both radiation-induced loss mechanisms exist simultaneously; therefore, radiation-induced loss is the result of joint action of the two. (4) Radiation-induced fluorescence density along the optical fiber axis is so low that measurement system with higher sensitivity is needed (e.g. photoelectric multiple tube). Taking the advantage of effects of radiation, on the one hand scientists can seek methods for decreasing additional loss and develop anti-radiation optical fibers suitable for transmission systems under radiation environments, and on the other hand they can also manufacture radiation dose meters based on this effect.

7. Acknowledgment

8. References

Akira I. and Junich T.(1988). Radiation resistivity in silica optical fibers[J]. *IEEE Journal of Lightwave Technology*. vol. 6(2), pp. 145-149, ISSN 0733-8724

An Y. Y., Liu J. F., Li Q. H., et al.(2002). *Optoelectronic Technology*[M]. Beijing: Electronic Industry Press, pp.117-120, ISBN 7-5053-7565-2 (in Chinese)

Evans B. D., Sigel G. H. & Jr.(1974). Permanent and transient radiation-induced loss in optical fibers[J]. *IEEE Transactions on Nuclear Science*. vol. NS-21, pp. 113-118, ISSN 0018 9499

Friebele E. J., Sigel G. H. & Jr.(1978). Radiation response of fiber optic waveguides in the 0.4 to 1.7μm region[J]. *IEEE Transactions on Nuclear science*. vol. NS-25(6), pp. 1261-1266, ISSN 0018-9499

Friebele E. J.(1979). Optical fiber waveguide in radiation environments[J]. *Optical Engineering*. vol. 18(6), pp. 552-561, ISSN 0091-3286

Friebele E. J., Lyon P. B., Blackburn J., et al.(1990). Interlaboratory comparison of radiation-induced attenuation in optical fibers. Part Ш: Transient exposures[J]. *IEEE Journal of Lightwave Technology*. vol. 8(6), pp. 977-989, ISSN 0733-8724

Fernadndez A., Berghmans F., Brichard B., et al.(2002). Toward the development of radiation- tolerant instrumentation data links for thermonuclear fusion experiments[J]. *IEEE Transactions on Nuclear Science*, vol. 49(6), pp.2879-2887, ISSN 0018-9499

Golob J. E., Lyon P. B. & Looney L. D.(1977). Transient radiation effects in low-loss optical waveguides[J]. *IEEE Transactions on Nuclear science*. vol. NS-24(6), pp. 2164-2168, ISSN 0018-9499

Ghoniemy S., Maceachern L., Mahmond S.(2003). Extended robust semiconductor laser modeling for analog optical link simulations[J]. *IEEE Journal of Selected Topics in Quantum Electronics*, vol. 9(3), pp.872-878, ISSN 1077-260X

Huang D. X.(1994). *Semiconductor optoelectronics*[M]. Chengdu: Electronics Science and Technology University Press, pp.144-153, ISBN 7-81016-151-2 (in Chinese)

Hinojosa J.(2001). S-parameter broadband measurements on-coplanar and fast extraction of the substrate intrinsic properties[J]. *IEEE Microwave and Wireless Components Letters*, vol. 11(2), pp.80-82, ISSN 1531-1309

Liu S. H.& Li C. F.(2006). Optoelectronic technology and application [M] Guangzhou, Hefei: Guangdong Science and Technology Press, Anhui Science and Technology Press. pp.800-801, ISBN 7-5359-4186-9 (in Chinese)

Mei Z. Y.(1966). *Nuclear Physics*[M].Beijing: Science Press. pp. 1-36 (in Chinese)

Mattern P. L., Watkins L. M., Skoog C. D., et al. (1974). The effects of radiation on the absorption and luminescence of fiber optic waveguides and material[J]. *IEEE Transactions on Nuclear Science*. vol. NS-21, pp. 81-95, ISSN 0018-9499

Moss C. E., Casperson D. E., Echave M. A., et al.(1994). A space fiber-optic X-ray burst detector[J]. *IEEE Transactions on Nuclear Science*. vol. 41(4), pp. 1328-1332, ISSN 0018-9499

May M. J., Clancy T., Fittinghoff D., et al.(2006). High bandwidth data recording systems for pulsed power and laser produced plasma experiments[J]. *Review of Scientific Instruments*, vol. 77(10), pp.1032-1035, ISSN 0034-6748

Pocha M. P., Golddard L. L., Bond T. C., et al.(2007). Electrical and optical gain level effects in InGaAs double quantum-well diode lasers[J]. *IEEE Journal of Quantum Electronics*, vol. 43(10), pp.860-868, ISSN 0018-9197

Ramsey A. T., Adler H. G. & Hill K. W.(1993). Reduced optical transmission of SiO2 fibers used in controlled fusion diagnostics[R]. *DE93008516*

Tsunemi K., Naoki W., Kazuo S., et al.(1986). Radiation resistance characteristics of optical fibers[J]. *IEEE Journal of Lightwave Technology*. vol.4(8), pp. 1139-1143, ISSN 0733-8724

Tighe W., Adler H., Cylinder D., et al.(1995). Proposed experiment to investigate use of heated optical fibers for Tokamak diagnostics during D-T discharges[R]. *DE95007355*

Tanaka T, Hibino Y., Hashimoto T., et al.(2002). Hybrid-integrated external-cavity laser without temperature-dependent mode hopping[J]. *IEEE Journal of Lightwave Technology*, vol. 20(9), pp.1730-1739, ISSN 0733-8724

Yasuo K. *Light-wave Engineering*[M]. Kyoritsu Shuppan Co., Ltd. and Science Press, pp.131-137, ISBN 7-03-010186-3, Beijing (in Chinese)

Zivojinovic P., Lescure M. & Tap-Béteille H.(2004). Design and stability analysis of a CMOS feedback laser driver[J]. *IEEE Transactions on Instrumentation and Measurement*, vol. 53(1), pp.102-108, ISSN 0018-9456
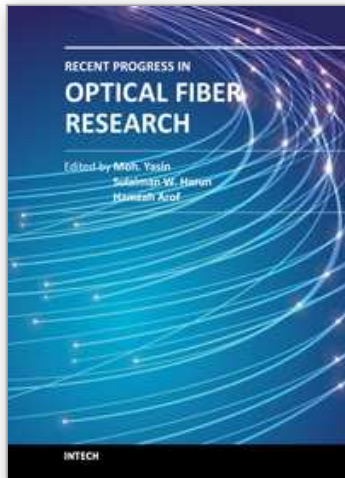
Recent Progress in Optical Fiber Research

Edited by Dr Moh. Yasin

This book presents a comprehensive account of the recent progress in optical fiber research. It consists of four sections with 20 chapters covering the topics of nonlinear and polarisation effects in optical fibers, photonic crystal fibers and new applications for optical fibers. Section 1 reviews nonlinear effects in optical fibers in terms of theoretical analysis, experiments and applications. Section 2 presents polarization mode dispersion, chromatic dispersion and polarization dependent losses in optical fibers, fiber birefringence effects and spun fibers. Section 3 and 4 cover the topics of photonic crystal fibers and a new trend of optical fiber applications. Edited by three scientists with wide knowledge and experience in the field of fiber optics and photonics, the book brings together leading academics and practitioners in a comprehensive and incisive treatment of the subject. This is an essential point of reference for researchers working and teaching in optical fiber technologies, and for industrial users who need to be aware of current developments in optical fiber research areas.

How to reference

In order to correctly reference this scholarly work, feel free to copy and paste the following:

Fuhua Liu, Yuying An, Ping Wang, Bibo Shao and Shaowu Chen (2012). Effects of Radiation on Optical Fibers, Recent Progress in Optical Fiber Research, Dr Moh. Yasin (Ed.), ISBN: 978-953-307-823-6, InTech, Available from: http://www.intechopen.com/books/recent-progress-in-optical-fiber-research/effects-of-radiation-on-optical-fibers

INTECH
open science | open minds